Liquid Mn Sintering of Plasma-Sprayed Ceramic Coating†

Akira OHMORI*, Zhan ZHOU* and Katsunori INOUE**

Abstract

The penetration phenomena of liquid Mn into porous Al_2O_3 and ZrO_2 (8wt%Y_2O_3) coatings, plasma-sprayed on SS400 steel substrate were studied by heating at 1573 °K in a vacuum atmosphere, and the possibility of improving the mechanical properties of Al_2O_3 and ZrO_2 coatings by heat-treatment with liquid Mn was examined. It was found that liquid Mn rapidly penetrated the ceramic coatings at the interface between the coating and the substrate. The densification of the coating occurred when Al_2O_3 and ZrO_2 particles were sintered with liquid Mn that penetrated the porous coatings. For Al_2O_3 coatings, the formation of $MnAl_2O_4$ was clearly recognized in the connected porosities of Al_2O_3 coatings penetrated by liquid Mn. In the case of ZrO_2 coatings, a dense coating was obtained by the sintering reaction between deposited ZrO_2 particles and the liquid Mn. The mechanical properties, such as the hardness and the fracture stress, of both Al_2O_3 and ZrO_2 coatings heat-treated with liquid Mn were greatly improved, compared with as-sprayed coatings. Moreover, the modulus of elasticity and the fracture toughness of the ZrO_2 coating reached the same levels as those of sintered PSZ(Y_2O_3)

KEY WORDS: (Al_2O_3 coating) (ZrO_2 coating) (Liquid manganese) (Sintering) ($MnAl_2O_4$) (Structural properties)

1. Introduction

Plasma-Sprayed ceramic coatings have been widely applied in many industrial fields because of the excellent wear, erosion, heat resistance, and corrosion resistance which ceramics themselves possess. Plasma-sprayed Al_2O_3 coatings are well known as wear and insulation coatings.[1] ZrO_2 stabilized with Y_2O_3 is well known as a thermal barrier coating.[2,3] However, because Al_2O_3 and ZrO_2 coatings, like all ceramics coatings, include connected porosities, properties such as mechanical strength, fracture toughness, wear resistance are greatly reduced. Nor do ceramic coatings play an important role in protecting the metal substrate in a corrosive atmosphere under high temperature conditions. To improve the properties of the coatings, various mesures have been reported,[4-6] such as sealing with resin, chromium trioxide and electro-plating. However, to make greater use of ceramic coatings at high temperature, it is necessary to develop more effective post-treatment methods.

In this study, the penetration of liquid Mn into connected porosities in Al_2O_3 and ZrO_2 coatings was utilized to form a dense, non-porous layer that improved the properties of the coatings. The penetration behavior of liquid Mn, and the mechanical properties of the improved coatings after liquid-Mn treatment were examined.

2. Materials and Experimental Procedures

The substrates were of JIS SS400 mild steel 15 x 15 x 3(mm), whose surface was grit blasted before spraying. Commercially available Al_2O_3 and ZrO_2 containing 8wt%Y_2O_3 as a stabilizer (Shoden K-90) was used as the spraying powder, whose mean particle size was 10-40μm. Plasma spraying was carried out in the air and Al_2O_3 coatings with a thickness of 150-200μm and ZrO_2 coatings with a thickness of 100-1000μm were produced. 99.99wt% Mn plates weighing about 3-5g were used for the penetration treatment. These assembles were ultrasonically degreased in acetone before heat-treatment. To compare the mechanical properties of ZrO_2 coatings heat-treated with liquid Mn, we used sintered, partially stabilized zirconia (PSZ) plates stabilized with 9.7 and 13wt%Y_2O_3 (Nikato, ZR6-Y and ZR-8Y).

Figure 1 shows a schematic diagram of the experimental apparatus for the liquid manganese

† Received on July 21, 1995
* The Advanced Materials Processing Institute Kinki Japan
** Professor

Transactions of JWRI is published by Welding Research Institute of Osaka University, Ibaraki, Osaka 567, Japan.

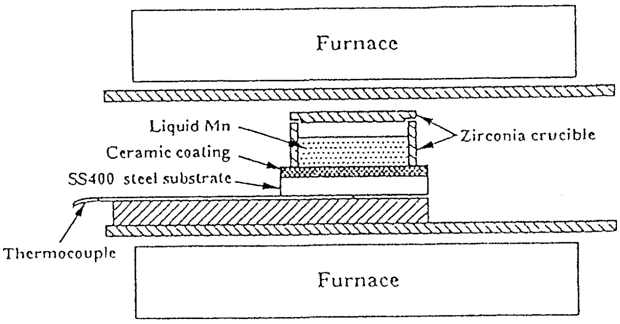

Fig. 1 Schematic diagram of the experimental apparatus for liquid Mn penetration treatment.

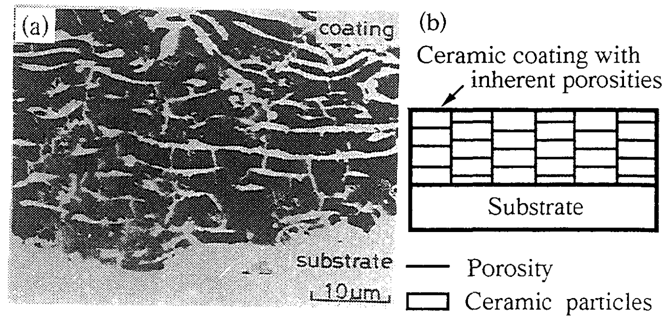

Fig. 2 (a)Typical SEM microstructure of a copper-electroplated Al_2O_3 coating. White strings are copper and represent vertical cracks in individual lamellaan. and non-bonded interfaces between flattened particles and (b) schematic illustration of cross-section of ceramic coating.

penetration treatment. The ZrO_2(8mol.%Y_2O_3) crucible with a 13-mm inside diameter and the Mn plate were set on the surface of ZrO_2 coatings. Definite quantities of manganese were placed in contact with the Al_2O_3 and ZrO_2 coating surfaces, then heated under a vacuum of 1.33 x 10-3 Pa at 1573°K at a rate of 56°K/min. After holding at the appointed temperature, the assembly cooled in the furnace at a rate of 1.5°K/min.

Cross-sections of as-sprayed Al_2O_3 and ZrO_2 coated test pieces and Al_2O_3 and ZrO_2 coated test pieces heat-treated with liquid Mn were examined by scanning electron microscopy (SEM). Changes in the elemental composition of the cross-section and crystal structure of the coating were studied by means of an electron probe micro analyzer (EPMA) and X-ray diffraction analysis (XRD), respectively. The fracture toughness of the densified coating heat-treated with liquid Mn and sintered zirconia employed by Niihara's equation[7], using the Indentation-Fracture method [IF], where the indentation load was 98 N for 20s.

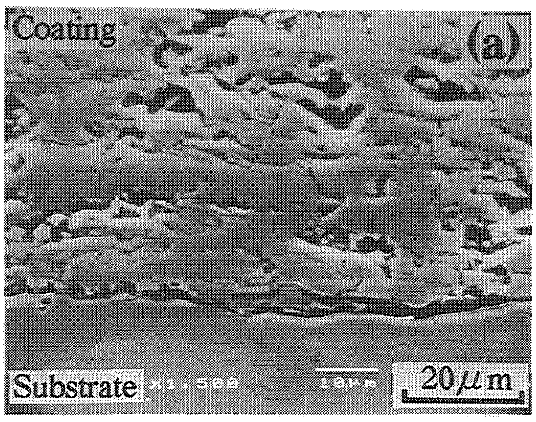

Fig. 3 Typical SEM microstructure of ZrO_2(8wt%Y_2O_3) coating.

3. Results and Discussion

Plasma-sprayed ceramic coatings have a layer structure formed by the deposition of flattened, rapidly solidified particles. Connected porosities exist in as-sprayed coatings and are composed of micropores, which are nonbonded areas between the ceramic lamellae and microcracks in individual flattened particles.[8] **Figure 2(a)** shows a typical SEM microstructure in the cross-section of the copperelectro-plated Al_2O_3 coating. The distribution of the connected porosities, the non-bonded areas between flattened particles and the vertical crack in individual flattened particles in the coating can all be observed. The diameter of these vertically and horizontally oriented porosities, in the as-sprayed Al_2O_3 coating are about 0.16-0.19μm and 0.25-0.38μm respectively. A schematic diagram of the distribution of the connected porosities from the coating surface to the interface between the coating and substrate is similar to the network shown in **Fig. 2(b)**.

Figure 3 shows a typical SEM microstructure in the cross section of the ZrO_2 coating. The diameter of these vertically and horizontally oriented porosities, in the as-sprayed ZrO_2 coating are about 0.3-0.5μm and 0.17-0.3μm, respectively.

Figure 4 shows the microstructure and EPMA line analysis results in the cross section of an Al_2O_3 coating heat-treated with Mn for 3.6ks at 1573°K in 1.33 x 10-3Pa. From this EPMA analysis,the Mn concentration in dense layers on the surface and at the interface of the coating is higher than that of the inside of the coating, and the intensity ratio between Mn and Al in both layers is almost same.

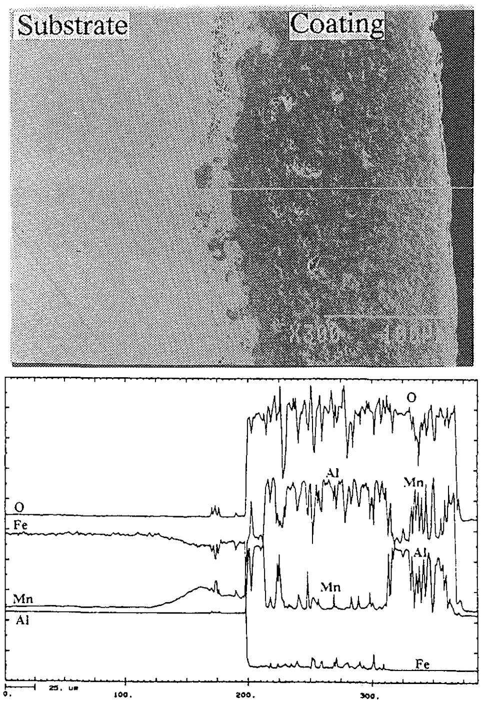

Fig. 4 SEM image and EPMA line analysis results of cross-section of Al_2O_3 coating heat-treated with Mn for 3.6ks at 1573°K in 1.33 x 10-3 Pa.

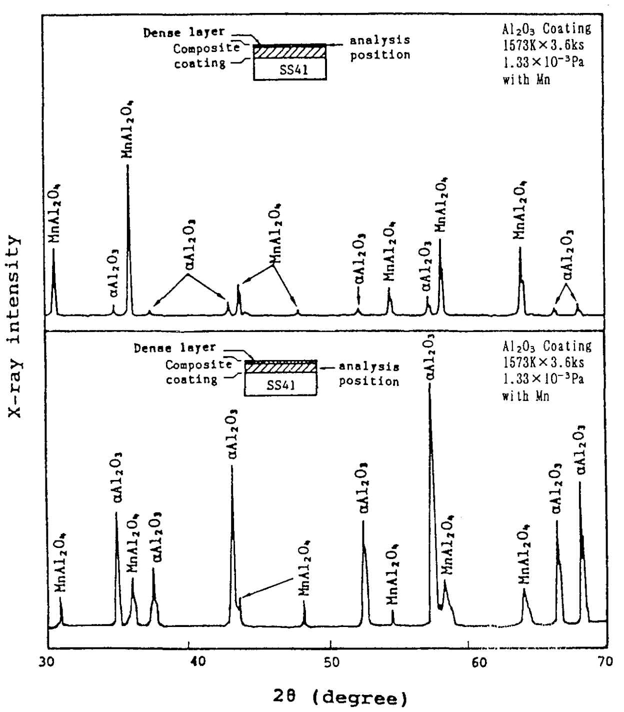

Fig. 5 XRD results of surface and interior of Al_2O_3 coatings heat-treated with Mn for 3.6ks.

On the inside of the coating, almost uniformly alternate changes of concentration of Mn and Al are recognized and narrow peaks of Mn exist between broad peaks of Al which shows the deposited Al_2O_3 particle part.

Figure 5 shows XRD results from the surface layer and the inside of the Al_2O_3 coating shown in Fig. 4. The $MnAl_2O_4$ on the new dense surface layer of the Al_2O_3 coating heat-treated with Mn was clearly recognized. The inside of the coating was composed of the Al_2O_3 phase and $MnAl_2O_4$ spinel. From this result, it is considered that $MnAl_2O_4$ spinel exists among the Al_2O_3 particles deposited. Moreover, the constant Mn concentration gradient from the coating side to the SS400 steel substrate is recognized and Mn-Fe alloy layer with a thickness of about 70μm was seen in the substrate side.

From these results, it was concluded that liquid Mn could penetrate easily the Al_2O_3 coating and it reached, in a short time,the interface between the coating and substrate through the connected porosities of the coating. The formation of $MnAl_2O_4$ by the reaction of Mn(O) and Al_2O_3 particle in the connected porosities increased with increase of heating time. The porosities in the Al_2O_3 coating were filled with $MnAl_2O_4$ spinel formed around Al_2O_3 deposited particles. On the other hand, a thick layer composed of $MnAl_2O_4$ as the main phase was formed on the surface of the Al_2O_3 coating due to the supply of a large amount of liquid Mn(O).

Figure 6 shows the results of SEM observation and line analysis of Mn by means of EPMA for a cross-section of the ZrO_2 coatings, heat-treated with Mn for 0.3ks(a) and 10.8 ks (b) at 1573°K at a pressure of 1.33 x 10^{-3} Pa. From the results of line analysis for Mn it was recognized that liquid Mn penetrated the surface of the ZrO_2 coatings and reached the interface between the SS400 substrate and ZrO_2 coating in as little as 0.3ks and, as the heat-treatment time increased, the concentration of Mn in the coating increased. After 7.2ks, Mn existed homogeneously throughout the ZrO_2 coating and was continuously distributed from the interior of the coating to the substrate, which may indicate that a chemical bond was formed in the interface between the coating and the substrate.

These results show that liquid Mn can easily penetrate the ZrO_2 coating surface and rapidly reach the interface between the substrate and the coating by following the connected porosities in the ZrO_2 coating. This penetration phenomenon of liquid Mn through the connected porosities of the ZrO_2 coating is due to the capillary tube phenomenon, and the wettability of ZrO_2 coatings by liquid Mn.

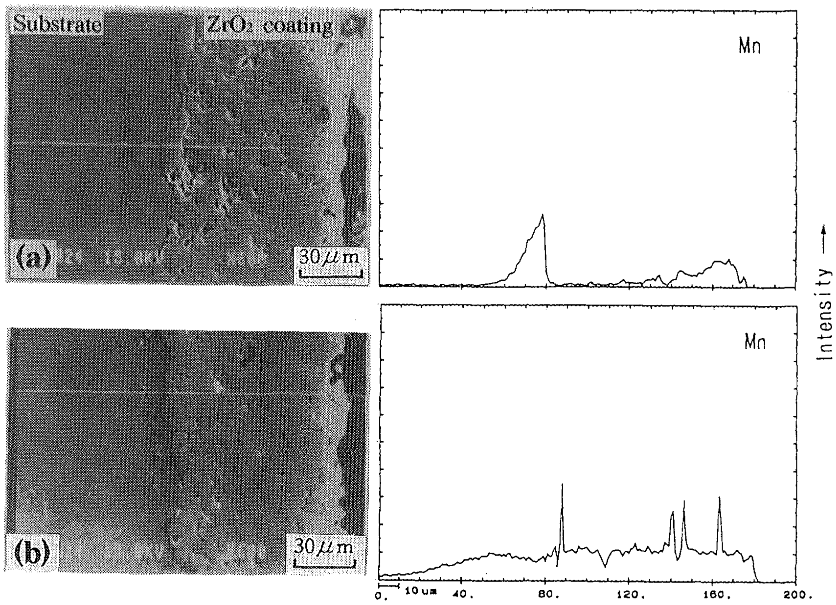

Fig. 6 SEM images and line analysis of Mn for cross-section of ZrO_2(8wt% Y_2O_3) oating heat-treated with Mn for 0.3ks (a) and 10.8ks (b) at 1573°K in a vacuum of 1.33 x 10^{-3}Pa.

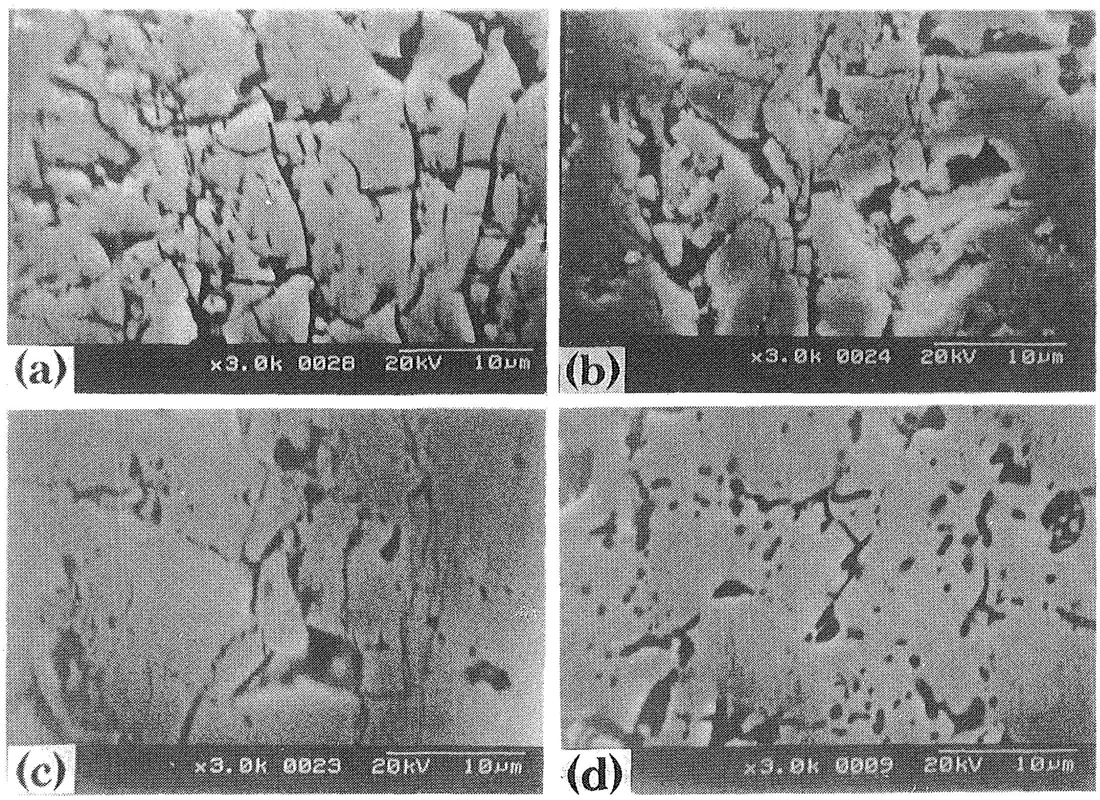

Fig. 7 Microstructure of the cross-section of ZrO_2 coatings: (a) as-sprayed ZrO_2 coating; (b) ZrO_2 coatings heat-treated for 10.8ks at 1573°K in a vacuum of 1.33 x 10^{-3}Pa; (c) and (d) ZrO_2 coatings heat-treated with Mn for 0.3 and 3.6ks, respectively, at 1573°K in a vacuum of 1.33 x 10^{-3}Pa.

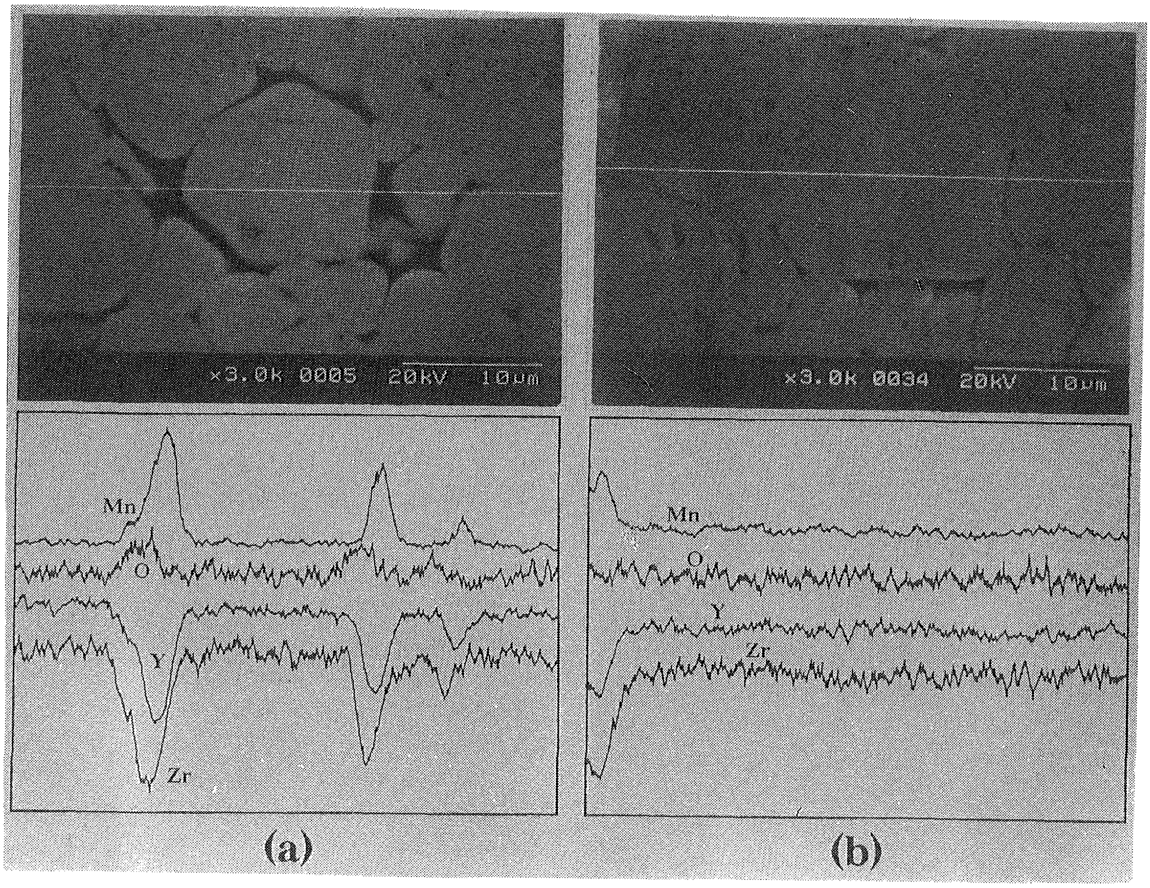

Fig. 8 Microstructure and line analysis results of Mn, Zr, O and Y for cross-sections of ZrO_2 coaings heat-treated with Mn at 1573°K in a vacuum of 1.33 x 10^{-3}Pa: (a) for 7.2ks, and (b) for 10.8ks.

Fig. 7 shows SEM enlargements of cross-sections of as-sprayed ZrO_2 coating(a), ZrO_2 coating heat-treated for 10.8ks at 1573°K under a vacuum of 1.33 x 10^{-3} Pa(b) and the microstructure change of ZrO_2 costings heat-treated with Mn for 0.3ks(c) and 3.6ks(d) at 1573°K under a vacuum of 1.33 x 10^{-3} Pa. In the figure, it can be seen that the structure in Fig.7(b) of ZrO_2 coating, heat-treated without Mn, resembles the structure of the as-sprayed coating shown in Fig. 7(a) but more cracks were produced in the coating. Therefore, the results show that effective sintering and densification among particles of the ZrO_2 coating can not be carried out under heat-treatment conditions without Mn. However, in the case of heat-treatment with Mn, the densification of the ZrO_2 coating was clearly seen in the SEM images shown in Fig.7(c) and (d), as the heat-treatment time increased from 0.3 ks to 3.6 ks. In the case of 0.3 ks, the existence of small separated particles can be seen in some regions. As the heat-treatment time was increased, the sintering progressed and the coatings consisted of the dense larger particles shown in Fig.7(d).

The final result of the coating densification is shown in **Fig.8**. The line analysis results of Mn, Zr, O and Y obtained by means of EPMA for a cross-section of the ZrO_2 coating heat-treated with Mn for 7.2 and 10.8 ks are also shown in this figure. In Fig.8(a), the structure consisting of flattened particles, seen in the as-coated structure or in the coating heat-treated with Mn for a short time, disappeared, and a structure with ball-shaped particles was formed below the surface of the coating. The grain boundaries between the particles consisted mainly of Mn and O. In the case of 10.8 ks (Fig.8(b)), these boundaries disappeared and all the elements were distributed with near uniformity on the particles and at the grain boundaries.

These results show that plasma-sprayed ZrO_2 coating can change to a dense coating after heat-treatment with liquid Mn and that the process of densification may be brought about by the penetration of liquid Mn into the coating and by sintering the ZrO_2 particles, through diffusion of Mn into the ZrO_2 particles.

The hardness of Al_2O_3-$MnAl_2O_4$ composite coatings after heat-treatment with Mn increased significantly, compared with about 7.0-8.0GPa, of the as-sprayed Al_2O_3 coating. Hardness of the Al_2O_3 composite coating in the case of heat-treatment with Mn for 10.8ks, reached about 16.0GPa, which is greater than about 14.5GPa for sintered Al_2O_3.

These results confirm that as-sprayed Al_2O_3 coatings with connected porosities become dense and the bond between deposited Al_2O_3 particles strengthened. The connected porosities in coatings were penetrated by liquid Mn(O) and were filled up with $MnAl_2O_4$ formed by the reaction of Al_2O_3 particle and liquid Mn(O). The hardness of ZrO_2 coatings after heat-treatment with Mn also increased significantly with an increase in the heat-treatment time, compared with about 6.8-7.8GPa, of the as-sprayed ZrO_2 coating. The hardness of a cross-section of a coating heat-treated with Mn for 10.8ks reached about 13.2GPa, its value being greater than approximately 10.3GPa for sintered PSZ(13wt%.Y_2O_3).

The fracture toughness of the ZrO_2 coating heat-treated with Mn was measured by the IF test, and compared with sintered PSZ. The fracture toughness can be obtained as follows.

$$Kc=0.203(C/a)^{-3/2} \cdot H \cdot a^{1/2} \quad (1)$$

$$H=1.8544P/(2a)^2 \quad (2)$$

Kc: fracture toughness; H: Vickers hardness; P: indentation load; C: half the average crack length; a: half the average length of the diagonal line of indentation.

In the IF test, the occurrence of median cracks at C/a>2.5 were recognized in the samples measured. **Figure 9** shows the fracture toughness measured for ZrO_2 coatings heat-treated with Mn for 7.2 and 10.8 ks at (1573°K, and for sintered PSZ (9.7wt%Y_2O_3) and PSZ (13wt%Y_2O_3). The fracture toughness of ZrO_2 coatings after heat-treatment with Mn increased as the heat-treatment time increased, and after heat-treatment for 10.8ks reached 3.7 $MN/m^{3/2}$, a value about equal to 3.8 $MN/m^{3/2}$, the fracture toughness of sintered PSZ 13wt%Y_2O_3). The difference in the fracture toughness of the ZrO_2 coatings after heat-treatment with Mn for 7.2ks and 10.8ks may be due to the difference in the amount of brittle Mn(O) present at the grain boundaries of the ZrO_2 particles. (Fig.8(a) and Fig.8(b))

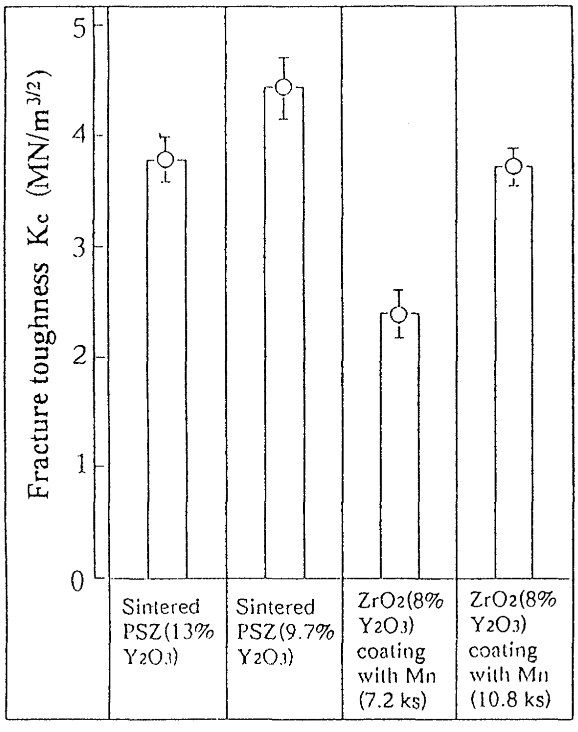

Fig. 9 Fracture toughness of ZrO_2 coatings heat-treated with Mn at 1573°K in 1.33 x 10-3Pa and PSZ.

4. Conclusion

Liquid-Mn penetration treatments of plasma-sprayed Al_2O_3 and ZrO_2 coatings were carried out in this study by heating in a vacuum to improve the mechanical properties of porous Al_2O_3 and ZrO_2 coatings. Mn penetration behavior into connected porosities in the coatings and the effect of coating densification were examined. The main results obtained are summarized below.

(1) During Mn penetration, liquid Mn(O) reacted with Al_2O_3 particles to form $MnAl_2O_4$. $MnAl_2O_4$ filled up the connected porosities in the Al_2O_3 coating.

(2) After heat-treatment with Mn, the density of the porous ZrO_2 coating was increased by the sintering action of liquid Mn that penetrated the interstices between the ZrO_2 particles in the ZrO_2 coating.

(3) It was recognized that Mn diffused into ZrO_2 particles during heat-treatment with Mn.

(4) The mechanical properties of Al_2O_3 and ZrO_2 coatings after heat-treatment with Mn were improved greatly, compared with those of as-sprayed coatings. The microhardness and fracture toughness of the ZrO_2 coating heat-treated for 10.8 ks reached 13.2 GPa and 3.7 $MN/m^{3/2}$, respectively, the same levels as the mechanical properties of sintered PSZ(13wt%Y_2O_3).

References

1) Arata, Y., Ceramic Spraying and Application, The Daily Industrial News Ltd., Japan 19 (1990).
2) Project 421-1, Final Report, Ceramic turbine components research and development, Part 2, EPRI Rep.AP-1539, August 1980 (Electric Power Research Institute).
3) Berndt C.C. and Herman H., Thin Solid Films,108, 427 (1983).
4) Miyajima K., Nomura N., Harada Y. and Nakahira H., J. High.Tepm Soc. Jpn. 18, 307 (1992).
5) Ohmori A., Li C.J. and Arata Y., Thin Solid Films, 201, 204 (1991) 241.
6) Arata Y., Ohmori A. and Li C.J., Trans. Jpn. Weld. Res. Inst. 17, 311 (1991).
7) Niihara K., Nakahira A. and Hirai T., Communications of the American Ceramic Society, 7 C-13(1984).
8) Ohmori A. and Li C. J., Thin Solid Films 201, 241 (1991).